https://doi.org/10.46861/bmp.28.307 PŮVODNÍ PRÁCE/ORIGINAL PAPER

Tectonic-thermal constraints on the Pb-Zn ore deposits from southeastern French Central Massif by K-Ar and Pb-Pb dating of illite

THEOFILOS TOULKERIDIS[1)]* AND NICOLE LIEWIG[2)]

[1)]*Universidad de las Fuerzas Armadas ESPE, Sangolquí, Ecuador; *e-mail: ttoulkeridis@espe.edu.ec*
[2)]*Institut Pluridisciplinaire Hubert Curien, 23 rue Becquerel, 67087 Strasbourg, France*

TOULKERIDIS T, LIEWIG N (2020) Tectonic-thermal constraints on the Pb-Zn ore deposits from southeastern French Central Massif by K-Ar and Pb-Pb dating of illite. Bull Mineral Petrolog 28(2): 307-321 ISSN: 2570-7337

Abstract

Illite-rich size-fractions (<0.2, <0.4, 0.4-1, 0.4-2 and <2 μm) of Cambrian, Permian, Triassic and Jurassic calcschists, shales and dolostones from Pb-Zn ore-district of the southeastern French Massif Central were dated by the K-Ar method, and some by the Pb-Pb method after removal of the Pb external to the illite particles. The combined mineralogical and isotopic determinations show that illitization occurred successively at 285 ± 5, 240 ± 20, 185 ± 15, 140 ± 10 and 105 ± 5 Ma in the district. These tectonic-thermal pulses, which were also reported at a larger regional scale, did not systematically release Pb-mineralizing fluids. The mineralizing episodes seem to have only contributed to contemporaneous illitization and Pb precipitation at 191 ± 41 Ma, by Pb-Pb dating of illite, and at 105 ± 5 Ma in a reactivated fault containing illite mixed with Pb precipitates. The scatter of the Pb-Pb data suggests an incompletely equilibrated Pb isotopic signature when incorporated into the illite structure during crystallization. Pb-isotopic determinations of barren illite-type minerals provide new information about the circulation timing of the mineralizing hydrothermal fluids. The fluid migrations related to recurrent hydrothermal activities occurred within a segment of a continental margin that was located away from main rift zones and far (more than 500 km) from major orogenic zones of Western Europe. The lack of major geodynamic activities near metal deposits needs to hypothesize periodic migrations of hot -fluids in the underneath continental crust. Metals were concentrated at specific places, but not necessarily during each tectonic -thermal pulse recorded by illite. These tectonic-thermal activities confirm local geodynamic re-activations of previously occurring events with effects on local mass and heat transfers in the plutonic basements, as well as in the sedimentary sequences.

Key words: *Pb-Zn ore district, southeastern French Central Massif, illite-type clays, K-Ar and Pb-Pb dating*

Received: 1. 6. 2020; accepted 17. 10. 2020

Introduction

Isotopic dating represents a basic parameter for reconstructing the genetic evolution of sediment-hosted ore deposits. However, such information is not necessarily straightforward as even recent analytical improvements have not removed all application uncertainties of isotopic methods applied to ore minerals. Such uncertainties can be due to lack of precise knowledge of the initial isotopic composition (Romer 2001), or to a tendency of ores to recrystallize easily in given environmental conditions, and therefore to potentially modify their elemental and isotopic compositions. Uranium minerals, for instance, contain large amounts of radiogenic Pb that allow routine application of the U-Pb dating method. However, their crystallization timing is sometimes questioned, because intermediate isotopes in the uranium decay chain are susceptible to escape from the mineral structures when exposed to subsurface conditions (Miller, Kulp 1963; Holliger et al. 1989; Misi et al. 1999).

In recent decades, indirect isotopic dating of ores has been promoted as a complementary approach to the isotopic dating of ore deposits by analyzing “barren” minerals that are associated with “ore” minerals and have expectedly crystallized at the same time as the ores (Clauer, Chaudhuri 1992). Among barren minerals often described within ore deposits are clay minerals that have dating potential by various isotopic methods as shown for long time (Ineson et al. 1975; Halliday et al. 1983; Toulkeridis et al. 1994; Toulkeridis et al. 1996; Toulkeridis et al. 1998; Zhao et al. 1999).

However, the information from such studies should go beyond the strict comparison of the ages of ore and associated barren minerals, as it should also be in the identification and quantification of the parameters impacting the evolution of an entire ore deposit. Clays have the advantage, which may also be a drawback sometimes, to be sensitive to discretely changing chemical and/or thermal conditions that can occur during a regional tectonic-thermal evolution of an economic metal-rich deposit (Clauer, Chaudhuri 1995).

Easily identified by appropriate methods including X-ray diffraction and electron microscopy, their study also has inconveniences, as it is often difficult to separate the authigenic from detrital material even by sophisticated separation methods. For instance, many studies on clay minerals associated with uranium deposits have pointed to the interest of such a combined geochronological approach (Lee, Brookins 1978; Bell 1985; Clauer et al. 1985;

Bray et al. 1987; Brockamp et al. 1987; Turpin et al. 1991; Rajesh 2008).

Studies on stable and radioactive isotope compositions of clay minerals from uranium deposits have highlighted how thermal and chemical information from associated barren minerals can sustain and even improve understanding of the evolution of the ore concentrations (Halter et al. 1987; Wilson et al. 1987; Kotzer, Kyser 1995; Kyser et al. 2000; Polito et al. 2006; Laverret et al. 2010; Goldfarb et al. 2010). Since age discordances are still reported in both the ore and associated barren mineral populations, a more detailed examination of the genetic relationship of both mineral types seems appropriate. This has been the case in particular in order to sort out if the tectonic-thermal evolution of a larger ore region is recorded by all ore precipitations. This occurred also when some of the identified events were not recorded because the interactive fluids were not systematically metal loaded. The use of clay minerals for complementary geochronological information of ore deposits has emphasized an important aspect, which is that clay minerals are able to record any hydrothermal activity. However, not all hydrothermal activity in an ore district necessarily induce ore concentrations (Clauer et al. 1992).

Therefore, in order to address independently such a regional evolution in the ore and associated clay minerals, the present study provides a K-Ar isotopic framework of illite from ore hosting rocks of different stratigraphic age, as well as from associated barren strata of the Pb-Zn mining district located in the southeastern French Massif Central, which are supplemented by Pb-Pb determinations on the same illite.

Geological setting and sampling

In the southeastern French Massif Central, the Paleozoic basement host-rocks, together with the Mesozoic sedimentary cover, represent a major inactive "metallogenic" province that produced about 2 millions of tons of Pb -Zn metals since the beginning of its exploitation (Fig. 1). In its northern part, the basement consists of late Variscan granites (Vialette, Sabourdy 1977; Hamet, Mattauer 1977), whereas the Causses-Shoal structural unit to the W and S resulted from a Triassic-to-Jurassic (Callovian) tectonic activity that induced faulting as well as changes in the sedimentation facies and rates of the Mesozoic sediments (Clauer et al. 1997). The whole district is located along the Cévennes faulting system, to the SE of the Massif Central, that has been active as a normal fault, at least during the Liassic extensional period (Lemoine 1984). The plutonic basement is overlain by Cambrian to Triassic dolomite-enriched black shales and Bathonian dolostones followed by Oxfordian shaly dolomites (Le Guen, Combes 1988).

Genesis of the regional Pb-Zn ore deposits is explained by various mineralizing processes, from karstic (Orgeval 1976; Connan, Orgeval 1977; Verraes 1983) to syngenetic (Macquar 1970; Michaud 1970) and diagenetic (Bernard 1958; Fogliérini et al. 1980), and by interactions with migrating hydrothermal fluids (Charef, Sheppard 1988; Ramboz 1989; Le Guen et al. 1991). Of special interest here is the study by Le Guen et al. (1991) who focused on the use of Pb isotopes to trace and constrain the genesis of the Pb-Zn ores. The Pb-Pb isotopic compositions of the different ore bodies appear quite homogeneous, ruling out a large contribution of external Pb during the successive concentration stages. In fact, such a model agrees well with the hypothesis of an initial stock of Pb that continued to evolve in an almost closed system at a regional scale, without significant gain of external Pb or loss of initial Pb.

Lancelot et al. (1995) reviewed the U-Pb and Pb-Pb data available on three major U deposits from French Massif Central: of the southeastern Lodève, central Bertholène and northern Pierres Plantées concentrations. The results suggest a generalized Liassic precipitation of the metallic ores and a common multi-stage evolution. Despite the diversity of the host rocks, such as Permian sediments above the unconformity with the Variscan basement at Lodève, the orthogneissic and mylonitic Variscan basement at Bertholène, and episyenitic veins cutting post-tectonic Variscan leucogranites at Pierres Plantées, U-Pb and Pb-Pb data demonstrate the occurrence of

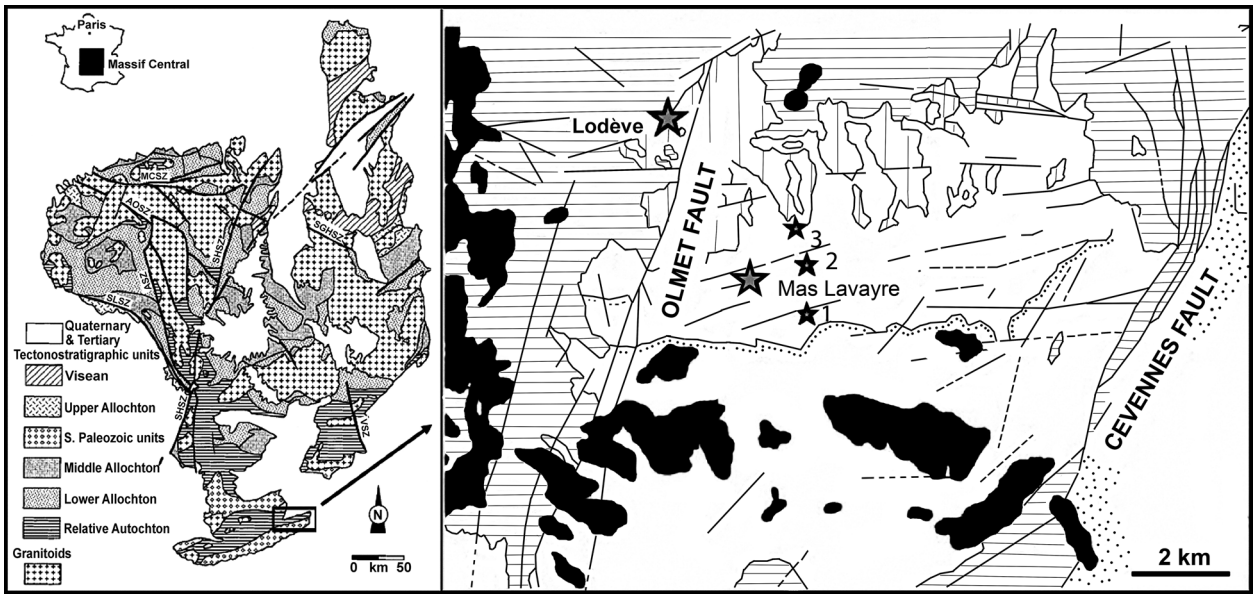

Fig. 1 *Geological overview of the French Massif Central (left) with the position of the Lodève district and the geographic distribution of the studied samples (right) from the Lodève district (modified from Merignac, Cuney 1999 and Santouil 1980). The stars 1, 2 and 3 to the east of Mas Lavayre locate the three drillings CTL, MLV and MRD, respectively.*

a major phase of U mobilization and concentration during Liassic time. These most likely are related to circulations of fluids at temperatures from 140 to 250 °C and salinities from 5 to 14% NaCl eq. At Pierre Plantées, a pre-concentration episode was identified at about 270 Ma in leucogranite veins percolated by fluids at 300 - 350 °C. At Bertholène, U concentration occurred at about 170 Ma as tiny spherules disseminated in predominant Oligocene coffinite. Further U remobilization was detected at Lodève and Pierres Plantées during the Cretaceous, which was locally confirmed by K-Ar dating of clay material from the Saint-Julien fault gouge containing U minerals (Mendez Santizo et al. 1991).

The clay material studied here was extracted from thirty-eight Cambrian, Permian, Triassic and Jurassic sedimentary samples of mines and exploration drillings near Lodève and Les Malines (Fig. 1 and 2; Table 1). Among twelve Cambrian calcareous schists, six were collected in the Montdardier mine located about 3 km to the W of Les Malines, one at an outcrop on top of the mine, and two from cores of exploration wells located about 2 km to the W of the mine. Two argillaceous dolostones were collected in Les Malines mine and another at the nearby Sanguinède mine excavated in black calcareous schists about 2 km to the NW of the Montdardier mine. From fifteen Autunian samples collected in the Mas Lavayre mine at about 5 km to the SE of Lodève, six belong to a limited transect across the Saint-Julien fault visible in the mine, and five to cores of three nearby wells on a N-S trajectory at 1 km to the E of Mas Lavayre (Fig. 1). Five authigenic feldspar splits were separated and purified from interlayered pyroclastic to tuffaceous beds in the Autunian sediments of the Mas Lavayre mine, and dated by the K-Ar method. Three Triassic shales were taken from cores of exploration drillings located at Tudes and Cozes; two are not mineralized at all and were selected purposely as references for the barren environment to be compared to the ore-rich material. Six Jurassic dolostones belong to exploration wells near Trèves at 27 km to the NW of Les Malines, with two argillaceus dolostones collected at Lanuejols at about 9 km to the N of Trèves.

Analytical procedure

The <2 μm size fractions were extracted from whole-rock samples after gentle hand grinding in an agate bowl, dispersion in de-ionized water and recovery by routine sedimentation following Stoke´s law. Additional size fractionations (<0.4, 0.4 - 2 μm) were conducted on the extracted <2 μm fractions by ultracentrifugation. The size fractions were investigated by powder X-ray diffraction (PXRD). The illite crystallinity index (ICI) of the 001 illite peak was determined following Kübler´s (1968; 1997) concept. Theoretically, ICI values below 0.25 define epizonal metamorphic conditions, values between 0.25 and 0.37 define anchizonal conditions, and higher values correspond to a diagenetic grade. The precise limits depend on the analytical conditions and the characteristics of the used XRD equipment (operated here at 40 kV/20 mA and equipped with a Cu anticathode and a Ni filter as well as slits of 1 and 2° on the side of the tube and the counter, respectively). Special attention was given to identify the potential occurrence of detrital minerals in the separated size fractions, such as micas and feldspars, as they potentially bias the isotopic ages of the authigenic clay fractions. Feldspar separates of varied sizes were obtained by freezing and thawing the tuffaceous samples, sizing them by wet-sieving, and by using high-density liquids for purification of the sized fractions. The separated size fractions were subjected to XRD, showing that they were never pure, but mixed with minute amounts of albite, quartz and muscovite. The two former have no impact on the K-Ar results, the occurrence of the latter was of some concern, so that only the size fractions devoid of muscovite were analyzed.

K-Ar determinations were made following Bonhomme et al.´s procedure (1975). The powders were preheated at 100 °C during 12 hours under vacuum to remove the atmospheric Ar adsorbed on the clay particles during sample preparation, handling, and clay separation. The accuracy of the Ar extraction method was periodically controlled by analysis of the international GL-O standard mineral which content in radiogenic ^{40}Ar averaged

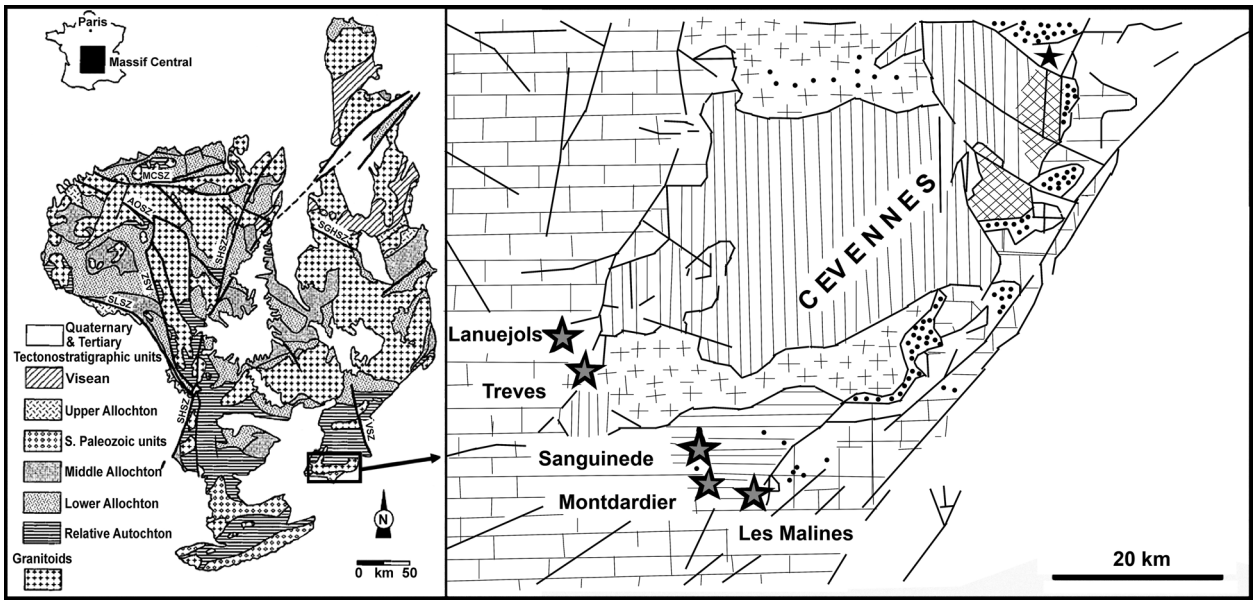

Fig. 2 *Position of the Les Malines district within the southeastern French Massif Central (left) and the geographic distribution (right) of the studied samples (modified from Merignac, Cuney 1999 and Santouil 1980).*

24.54 ± 0.15 × 10^{-6}cm^3 (2σ) for 4 independent analyses. The ^{40}Ar/^{36}Ar ratio of the atmospheric argon was also measured periodically, averaging 295.0 ± 1.9 (2σ) for 5 independent analysis, also during the course of the study. The results being analytically consistent and close to the theoretical values of 24.85 ± 0.24 × 10^{-6} cm^3 ^{40}Ar for the GL-O standard (Odin et al. 1982) and 295.5 for the atmospheric ^{40}Ar/^{36}Ar ratio (Nier 1950), no correction was applied to the raw data. The blank of the coupled extraction line and mass-spectrometer was also checked weekly before Ar extraction: below 10^{-8} cm^3 (routinely at about 0.8 × 10^{-8} cm^3), the amount of radiogenic ^{40}Ar was two orders of magnitude lower than the amounts of that extracted from samples, and therefore did not bias the data. The K contents were determined by flame spectrometry and the K-Ar ages calculated with the usual decay constants (Steiger, Jäger 1977). The overall precision of the K-Ar ages was estimated to be better than 2 %.

For an accurate examination of the Pb trapped by the clay particles, and therefore for its distinction from that adsorbed on the particle surfaces or sticking at the particles as oxide or sulfide crystals, the extracted clay particles were gently leached with dilute HCl. This procedure has been used for long in isotopic studies to analyze separately the elements adsorbed onto and those trapped in the clay particles (Nasraoui et al. 2000; Clauer et al. 2020). The selected clay fractions were leached during 15 minutes at room temperature with 1M HCl, centrifuged to recover and analyze separately the supernatant and the residue. This procedure is known to have no altering effect on the isotopic systems of the leached materials (Clauer et al. 1993). To ensure that no galena grains were sticking at the studied clay particles, the leached clay particles were observed by scanning-electron microscope (SEM); Pb-sulfide crystals were observed on the illite particles before leaching, never after. Lead was separated and purified on an ion-exchange resin conditioned with 0.6N HBr using Krogh´s (1973) technique. An aliquot of 150 ng of Pb was directly loaded with phosphoric acid and silica gel on a Re single-filament of a multi-collector mass-spectrometer (Cameron et al. 1969). Repetitive measurements of the standard NBS 982 indicated a mass discrimination correction of 0.18% per amu determined by repeat measurements of the standard (Todt et al. 1996).

Table 1 *Location, stratigraphic position and description of the studied samples*

Sample #	*Stratigraphy*	*Sample description*
Montdardier M1	Cambrian	Mine, eastern wall, argillaceous dolomite
Montdardier M2		Mine, northern wall, calcschist sampled 1 m below a pyrite layer
Montdardier M3		Mine, the same unit at the contact with the pyrite layer
Montdardier M4		Mine, the same location, pyrite layer
Montdardier M5		Mine, the same location, breccia at the top of the pyrite layer
Montdardier M6		Mine, sampled 1 m above M5, same facies
Montdardier MS1		Mine, excavation surface close to an important ore concentration
Montdardier F1		Core, mineralized sample from F18 drilling into an excavation
Montdardier F2		Core, sample from F19 drilling to the N of Montardier mine
Sanguinède S1		Mine, representative sample of the common black calcschist
Les Malines LM1		Mine, argillaceous dolomite with sphalerite in veinlets
Les Malines LM2		Mine, argillaceous dolomite in a cavity of Cambrian dolostones
Mas Lavayre ML1	Permian	Mine, greyish silt with some bituminous inclusions
Mas Lavayre ML2		Mine, grey-to-red sandy shale
Mas Lavayre ML3		Mine, redish pelite with bituminous stratiform accumulations
Mas Lavayre ML4		Mine, redish pelite
Mas Lavayre SJ1		Mine, eastern wall, Saint Julien fault, 1 m off a main fault
Mas Lavayre SJ2		Mine, eastern wall Saint Julien fault, 4 m away from the same fault
Mas Lavayre SJ3		Mine, eastern wall, Saint Julien fault, 1 m from a lateral fault
Mas Lavayre SJ4		Mine, eastern Saint Julien fault, within a lateral fault
Mas Lavayre SJ5		Mine, eastern wall, Saint Julien fault, 0.5 m off the same lateral fault
Mas Lavayre SJ6		Mine, eastern Saint Julien fault, 5 m from the same lateral fault
CTL (97m) CTL1		Core, barren pelite
MLV354 (94m) MLV1		Core, barren shale on top of a bituminous dolomitic shale
MLV354 (236m) MLV2		Core, sandy pelite
MLV354 (286m) MLV3		Core, dolomitic shale above an uraniferous bitumen concentration
MRD12 (120m) MRD1		Core, carbonateous and shaly layer
Tudes Tu1	Triassic	Core, barren green shale above Pb-Zn with gypsum and anhydrite
Tudes Tu2		Core, mineralized Upper-Triassic shale from a drilling nearby
Crozes C1		Core, barren sample taken away from any ore concentration
Lanuejols L1	Jurassic	Mine, mineralized dolostone with dissolution features
Lanuejols L2		Mine, 15 km to the N of Trèves, barren argillaceous dolostone
Treves Tr1		Mine, barren dolostone
Treves Tr2		Mine, barren dolomitized argillaceous limestone
Treves Tr3		Mine, argillaceous dolostone with fragments of ZnS
Treves Tr4		Mine, mineralized argillaceous dolostone
Treves Tr5		Mine, main mineralization in clay, quartz and dolomite
Treves Tr6		Mine, barren dolomitized argillaceous limestone

Results

The PXRD results

On the basis of the XRD results, the separated size fractions consist mainly of illite mixed with either chlorite (up to 80 - 90 % in two Permian samples) or little kaolinite (5 to 15% in three fractions) (Table 2). None of the fine <0.4 µm size fraction contained visible accessory (= contaminating) minerals such as micas and feldspars. Most ICI of the fine <0.4 µm fractions are below a value of about 0.36 (Table 2), with only the fraction of the Cambrian sample M1 yielding a higher ICI. Most of the values are within the epizonal and the lower anchizonal domain, suggesting crystallization temperatures of about 160 - 280 °C for the studied illite material (Kübler 1997).

The different size fractions of the F1 feldspar separates contained pyrite, pyrolusite, quartz and galena for the 80 - 100 mm fraction, quartz for the 125 - 200 µm fraction, and apatite, uraninite and quartz for the 200 - 400 µm fraction. The 125 - 200 µm fraction of the F2 feldspar separate contained pyrite, uraninite, quartz and pyrolusite.

The K-Ar data

At a first glance, the sixty-seven K-Ar data range widely from 298.3 ± 13.7 to 103.0 ± 3.5 Ma (Table 3). The K-Ar ages of the five feldspar separates cluster into two groups at 281 ± 2 Ma for three of them and at 254 ± 1 Ma for the two others. Among the illite ages, twenty-three were measured on <0.4 µm sub-fractions extracted and analyzed separately to evaluate if the bulk <2 µm fracti-

Table 2 *PXRD mineralogical data of the studied size fractions*

Sample #	*Size (µm)*	*Illite (%)*	*Kaolinite (%)*	*Chlorite (%)*	*Acc.*	*ICI*
Montdardier M1	<0.4	100	tr		-	0.50
	0.4 - 2	85	15		Q, F	0.29
Montdardier M2	<2	100			Q, F	0.23
Montdardier M3	<2	90	10		Q, F	0.27
Montdardier M4	<2	100			Q	0.36
Montdardier M5	<0.4	100			-	0.35
	0.4 - 2	100			Q, F	0.21
Montdardier M6	<2	100			Q, F	0.29
Montdardier DS1	<2	100			-	n.d.
Montdardier F1	<2	100			Q	n.d.
Montdardier F2	<2	100			-	n.d.
Sanguinède S1	<0.4	100	tr		-	0.26
	0.4 - 2	80		20	Q, F	0.30
Les Malines LM1	<2	100			trQ	0.28
Les Malines LM2	<2	100			eQ, F	0.30
Mas Lavayre ML1	<2	25 (+15I/S)		60	trF	n.d.
Mas Lavayre ML2	<2	55		45	Q, trF	n.d.
Mas Lavayre ML3	<2	35		65	Q, F	n.d.
Mas Lavayre ML4	<2	40 (+15I/S)		45	F	n.d.
Mas Lavayre SJ1*	<0.4	100				0.46
Mas Lavayre SJ2*	<0.4	0 (+70I/S)		30		n.d.
Mas Lavayre SJ3*	<0.4	60 (+10I/S)		30		n.d.
Mas Lavayre SJ4*	<0.4	35 (+50I/S)		15		n.d.
Mas Lavayre SJ5*	<0.4	70		30		0.52
Mas Lavayre SJ6*	<0.4	60		40		n.d.
CTL (97m) CTL1	<2	80		20	F	0.70
MLV354 (94m) MLV1	<2	80		20	F	0.45
MLV354 (236m) MLV2	<2	20		80	Q, F	n.d.
MLV354 (286m) MLV3	<2	10		90	F	n.d.
MRD12 (120m) MRD1	<2	100			Q, F	n.d.
Tudes Tu1	<2	90		10	-	n.d.
Tudes Tu2	<2	80		20	Q	n.d.
Crozes C1	<2	100			Q	n.d.
Lanuejols L1	<2	100	tr		trQ	0.95
Lanuejols L2	<2	100			Q	0.95
Treves Tr1	<2	100			trQ	1.30
Treves Tr2	<2	100			trQ	1.35
Treves Tr3	<2	90	10		trQ, trF	0.80
Treves Tr4	<2	100			Q, trF	0.87
Treves Tr5	<2	100			F	0.65
Treves Tr6	<2	100			Q, trF?	0.67

* data from Mendez Santizo (1990); I/S stands for illite/smectite mixed layer, F for feldspar, Q for quartz, tr for traces, n.d. for not determined, Acc. for accessory minerals and ICI for Illite Crystallinity Index.

ons were isotopically homogeneous or if they consisted of several generations of illite particles. Three of these samples yielded K-Ar ages within analytical uncertainty for their two analyzed size fractions: the Cambrian LM1 argillaceous dolomite from Les Malines with an average age of 289.3 ± 6.7 Ma, and two Autunian samples of the drillings MLV2 and MRD1 with respective average ages of 176.1 ± 3.0 and 202.8 ± 2.8 Ma. The <0.2 µm fraction was separated as well in three more samples. In two of them (samples SJ3 and SJ4) the values are also within analytical uncertainty at 136.1 ± 4.0 and 106.6 ± 3.5 Ma.

The coarser 0.4 - 2 µm size fractions of all other samples yield older K-Ar ages than the finer fractions, therefore consisting of heterogeneous material with detrital components, unless these older components crystallized during previous tectonic-thermal episodes. In any case, the detrital or the older authigenic illite populations increase the K-Ar ages of the analyzed finer illite fractions, and therefore bias their age. This is especially the case for the Jurassic samples of Lanuejols (L1) and Trèves (Tr1, Tr3, Tr5, Tr6), whose deposition time is systematically younger than 200 Ma, and which 0.4 - 2 µm fractions yield K-Ar ages that are systematically older than 200 Ma. Plotting the K-Ar ages of the illite <0.4 µm fractions and the feldspar separates, all considered to be geologically meaningful, in an age histogram relative to their depositional

Table 3a *K-Ar results of the studied illite-rich fractions and feldspar separates*

Sample #	*Fractions (µm)*	*K_2O (%)*	*Ar* (%)*	*$^{40}Ar^*$ (10^{-6} cm^3/g)*	*K-Ar age (Ma + 2 σ)*
Montdardier M1	<0.4	9.01	95.81	60.27	196.5 (4.2)
	0.4 - 2	8.21	96.65	67.32	238.0 (5.1)
Montdardier M2	<2	7.72	88.17	62.89	236.6 (6.6)
Montdardier M3	<2	7.87	66.25	78.79	286.7 (9.8)
Montdardier M4	<2	6.81	45.57	67.68	284.7 (13.3)
Montdardier M5	<0.4	8.77	94.90	73.59	243.2 (5.3)
	0.4 - 2	7.30	96.80	76.09	297.5 (6.4)
Montdardier M6	<2	6.97	46.40	72.85	298.3 (13.7)
Montdardier DS 1	<2	7.62	92.40	47.31	183.0 (4.1)
Montdardier F1	<2	7.01	87.80	48.44	202.6 (4.8)
Montdardier F2	<2	7.03	89.30	45.55	190.6 (4.4)
Sanguinède S1	<0.4	7.99	76.00	61.84	225.5 (6.1)
	0.4 - 2	6.99	69.60	65.34	269.0 (7.9)
Les Malines LM1	<0.4	6.16	54.74	60.72	282.6 (10.5)
	0.4 - 2	6.66	84.74	69.05	296.1 (7.3)
Les Malines LM2	<0.4	7.39	54.92	58.40	229.9 (8.5)
	0.4 - 2	7.87	86.83	79.11	287.7 (6.8)
Mas Lavayre ML1	<0.4	6.30	79.2	27.46	130.4 (3.9)
	0.4 - 2	6.05	90.5	36.35	177.4 (4.1)
Mas Lavayre ML2	<2	8.06	66.50	59.56	215.8 (6.6)
Mas Lavayre ML3	<2	4.43	46.70	29.62	196.4 (8.6)
Mas Lavayre ML4	<2	10.10	91.20	69.71	202.4 (4.5)
Mas Lavayre SJ2	<0.4	6.50	75.92	29.71	136.5 (3.7)
	0.4 - 1	6.56	86.45	38.96	175.5 (4.2)
Mas Lavayre SJ3	<0.2	6.36	71.65	28.07	132.0 (4.3)
	<0.4	6.43	78.07	30.24	140.3 (3.7)
	0.4 - 1	5.93	78.06	35.17	175.3 (4.7)
Mas Lavayre SJ4	<0.2	6.04	58.84	20.67	103.0 (3.5)
	<0.4	6.10	76.97	22.31	110.1 (3.0)
	0.4 - 1	6.36	76.93	31.23	146.3 (3.9)
Mas Lavayre SJ5	<0.4	6.93	85.73	46.80	198.3 (4.8)
	0.4 - 1	7.05	86.65	53.85	222.7 (5.3)
Mas Lavayre SJ6	<0.2	7.05	85.99	55.95	230.8 (6.5)
	<0.4	7.09	90.15	60.53	247.2 (5.7)
	0.4 - 1	6.85	89.70	65.92	276.3 (6.9)
CTL (97m) CTL1	<0.4	5.67	69.2	49.61	252.9 (8.4)
	0.4 - 2	4.71	65.0	46.56	283.3 (9.6)
MLV354 (94m) MLV1	<0.4	5.88	66.5	49.53	244.1 (8.3)
	0.4 - 2	4.98	75.5	48.20	277.8 (7.8)
MLV354 (236m) MLV2	<0.4	4.95	42.7	30.00	178.9 (8.7)
	0.4 - 2	5.84	54.3	38.81	195.2 (7.3)
MLV354 (286m) MLV3	<0.4	2.83	69.9	16.57	173.1 (7.5)
	0.4 - 2	2.56	85.4	15.53	179.1 (4.8)
MRD12 (120m) MRD1	<0.4	10.10	93.5	68.85	200.0 (4.4)
	0.4 - 2	11.92	97.1	83.64	205.6 (4.3)

*Ar stands for radiogenic Ar

ages, highlights four age clusters (Fig. 3). The first age cluster is an initial episode at 290 - 280 Ma consisting mostly of three feldspar ages and one Cambrian fraction, while the second reflects an episode with an extent of 220 - 260 or 240 - 260 Ma identified by three or one Cambrian fraction, four Permian fractions and two feldspar separates. Furthermore, a third episode at 170 - 200 Ma has been identified with one Cambrian fraction, four Permian, and five Jurassic fractions, as well as the U-Pb age of Cambrian illite that will be discussed in the next section. A final phase is given by two younger episodes at 140 ± 10 Ma in Permian fractions, and at 105 ± 5 Ma in the Saint-Julien fault.

The coarser (0.4 - 1, 0.4 - 2 and <2 μm) fractions of the Cambrian samples either range near the 280 - 300 Ma event or on the older side of the 180 - 200 Ma, confirming the reality of these episodes and showing also, conversely, that the 220 - 260 Ma and the 150 to 100-Ma events did not impact the Cambrian material. The old K-Ar ages of the coarse Permian samples are obviously biased by detritals as they are either similar to the deposition ages or older. Most of the other K-Ar ages of the Permian material are on the older side of the 170 - 190 Ma event, indicating some partial resetting. The coarse Triassic fractions yield K-Ar ages either in the 180 - 200 Ma period or slightly older (Table 3).

The Pb-Pb data

The Pb-isotopic data of the untreated size fractions show a narrow range for the $^{206}Pb/^{204}Pb$ ratio from 18.41 to 19.87, and relatively uniform $^{207}Pb/^{204}Pb$ and $^{208}Pb/^{204}Pb$ ratios of ~15.7 and ~38.3, respectively (Table 4). The calculated μ-values are relatively low (0.1 to 7.0), indicating an expected crustal origin and composition for Pb, as most Pb-isotope values plot along the Stacey, Kramer (1975) second stage evolution curve with a μ-value of ~9.8 (Table 4). The Pb-Pb field of the untreated clay material is close to that defined by the Pb isotope values of the Les Malines ores. The $^{206}Pb/^{204}Pb$ isotope values are negatively related to the Pb-concentrations, linking the

Table 3b *K-Ar results of the studied illite-rich fractions and feldspar separates*

Sample #	*Fractions (μm)*	*K_2O (%)*	*Ar* (%)*	*$^{40}Ar^*$ (10^{-6} cm^3/g)*	*K-Ar age (Ma + 2 s)*
Mas Lavayre feldspars					
Feldspar F1a	80 - 100	4.82	45.22	47.71	283.6 (13.0)
Feldspar F1b	100 - 125	5.45	52.43	53.38	280.9 (11.6)
Feldspar F1c	125 - 200	9.00	76.90	79.29	254.5 (7.5)
Feldspar F1d	200 - 400	7.36	62.18	64.82	254.5 (8.9)
Feldspar F2	125 - 200	9.56	85.32	93.67	281.0 (7.6)
Tudes Tu1	<2	6.81	85.20	41.33	179.1 (4.4)
Tudes Tu2	<2	6.65	86.20	42.69	188.9 (4.6)
Crozes C1	<2	4.44	83.90	30.85	203.6 (5.4)
Lanuejols L1	<0.4	6.71	84.82	42.11	184.9 (4.5)
	0.4 - 2	5.74	89.45	41.50	211.4 (5.0)
Lanuejols L2	<2	4.73	85.77	23.80	149.7 (3.7)
Treves Tr1	<0.4	7.25	91.89	42.99	175.2 (4.0)
	0.4 - 2	7.19	93.96	49.18	200.7 (4.5)
Treves Tr2	<2	9.57	91.81	37.87	118.8 (2.6)
Treves Tr3	<0.4	6.60	84.02	42.22	188.3 (4.7)
	0.4 - 2	6.75	90.75	51.70	223.3 (5.2)
Treves Tr4	<2	7.53	72.39	32.81	130.3 (3.7)
duplicate			69.60	32.59	129.5 (3.8)
Treves Tr5	<0.4	5.40	86.78	33.36	182.2 (4.5)
	0.4 - 2	4.60	88.72	31.85	203.0 (5.0)
Treves Tr6	<0.4	6.25	64.71	38.34	181.0 (5.7)
	0.4 - 2	4.02	77.93	29.48	214.3 (5.9)

*Ar stands for radiogenic Ar

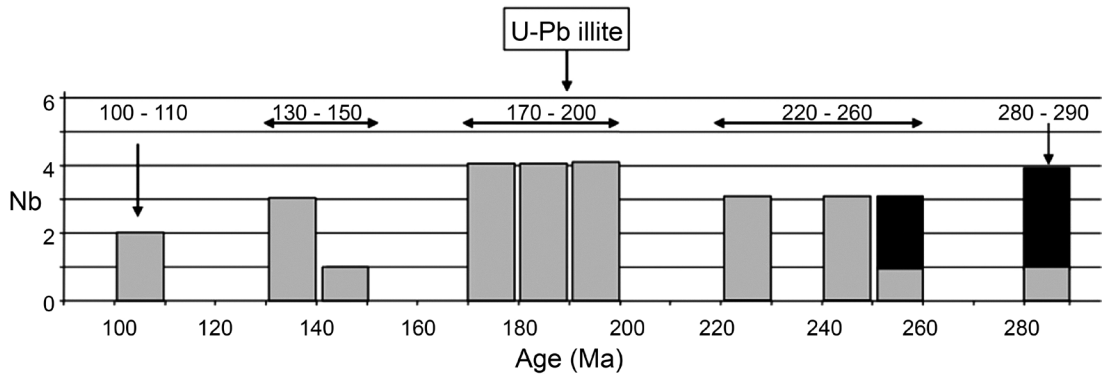

Fig. 3 *K-Ar histogram of the fine <0.4 mm illite fractions and the feldspar separates. The grey boxes correspond to the illite fractions and the black ones to the feldspar separates.*

highest Pb-concentrations to the most primitive (lowest) $^{206}Pb/^{204}Pb$ isotope values. The data points of the clay residues after leaching plot significantly above the fields of the major suppliers of the ore deposits (Table 5; Fig. 4), along an array giving an age of 191 ± 41 Ma.

Leaching of the <2 µm clay fractions allowed separate analysis of the Pb from dilute HCl-soluble mineral phases adsorbed onto the clay particle surfaces. Ten data points of the leachates plot along an array in the $^{207}Pb/^{204}Pb$ vs. $^{206}Pb/^{204}Pb$ diagram, which again has not the characteristics of an isochron, but those of an errorchron. Its slope provides an age of 568 ± 44 Ma (Table 5; Fig. 5).

Table 4 *Pb, Th and U concentrations and Pb isotopic compositions of the studied clay fractions and µ, κ, ω calculated ratios*

Sample #	Fractions (µm)	$^{206}Pb/^{204}Pb$	$^{207}Pb/^{204}Pb$	$^{208}Pb/^{204}Pb$	Pb (mg/g)	Th (mg/g)	U (mg/g)	U/Pb	µ	κ	ω
Montd. M1	<0.4	19.529	15.829	36.805	94.15	10.77	6.43	0.188	4.298	0.031	7.439
	0.4 - 2	19.338	15.696	38.313	227.8	21.15	9.42	0.354	2.644	0.019	6.135
Montd. M2	<2	19.867	15.710	38.304	70.75	4.98	7.71	0.532	7.024	0.051	4.686
Montd. M3	<2	18.601	15.657	38.356	215.9	5.17	7.68	0.279	2.253	0.016	1.568
Montd. M4	<2	18.480	15.675	38.453	492.2	7.82	10.95	0.064	1.409	0.010	1.040
Montd. M5	<0.4	18.722	15.679	38.364	977	11.18	13.75	0.098	0.894	0.006	0.751
	0.4 - 2	18.726	15.771	38.624	500	8.09	11.98	0.073	1.527	0.011	1.065
Montd. M6	<2	19.324	15.636	38.268	149.8	6.52	11.99	0.264	5.110	0.037	2.872
Montd. MS1	<2	18.514	15.670	38.482	123.3	19.33	4.26	0.097	2.189	0.016	10.26
Montd. F1	<2	18.416	15.674	38.451	2177	14.57	5.97	0.011	0.173	0.001	0.438
Montd. F2	<2	18.649	15.655	38.351	123.6	8.55	4.88	0.175	2.499	0.018	4.531
Sang. S1	<0.4	19.111	15.691	38.187	86.02	9.71	8.61	0.365	6.373	0.046	7.423
	0.4 - 2	19.137	15.548	37.550	150.4	9.82	11.10	0.412	4.652	0.034	4.252
Tudes Tu1	<2	19.362	15.681	38.631	73.51	12.49	7.62	0.271	6.657	0.048	11.28
Tudes Tu2	<2	18.413	15.705	38.551	3602	16.35	6.17	0.008	0.109	0.001	0.297
Crozes C1	<2	18.731	15.668	38.388	128.1	16.41	5.43	0.235	2.693	0.020	8.405

Table 5 *Pb isotope compositions of the leachates and residues from the studied size fractions*

Sample #	Fractions (µm)	$^{206}Pb/^{204}Pb$ (±2σ)	$^{207}Pb/^{204}Pb$ (±2σ)	$^{208}Pb/^{204}Pb$ (±2σ)
Residues				
Montdardier M1	<2	20.616 (0.004)	15.732 (0.004)	39.356 (0.014)
	<0.4	19.853 (0.002)	15.736 (0.002)	38.956 (0.014)
	0.4 - 2	19.775 (0.001)	15.724 (0.001)	38.989 (0.002)
Montdardier M2	<2	20.663 (0.001)	15.776 (0.001)	38.505 (0.001)
Montdardier M3	<2	18.877 (0.004)	15.736 (0.004)	38.653 (0.011)
Montdardier M4	<2	18.496 (0.007)	15.716 (0.005)	38.594 (0.012)
Montdardier M5	0.4 - 2	18.640 (0.019)	15.755 (0.018)	38.716 (0.061)
Montdardier M6	<2	19.445 (0.002)	15.723 (0.002)	38.629 (0.005)
Sanguinède S1	<2	33.807 (0.005)	17.087 (0.003)	39.184 (0.006)
	<0.4	20.478 (0.002)	15.760 (0.002)	38.846 (0.004)
	0.4 - 2	20.862 (0.002)	15.800 (0.002)	38.996 (0.005)
Leachates				
Montdardier M1	<2	19.067 (0.003)	15.698 (0.002)	38.365 (0.005)
	duplicate	19.062 (0.003)	15.695 (0.002)	38.352 (0.005)
	<0.4	19.221 (0.001)	15.689 (0.001)	38.092 (0.001)
	0.4 - 2	19.095 (0.002)	15.677 (0.001)	38.068 (0.003)
Montdardier M3	<2	18.496 (0.001)	15.642 (0.001)	38.313 (0.001)
Montdardier M4	<2	18.438 (0.003)	15.659 (0.004)	38.438 (0.011)
Montdardier M5	<2	18.404 (0.001)	15.628 (0.001)	38.318 (0.001)
	duplicate	18.393 (0.003)	15.637 (0.003)	38.367 (0.010)
	0.4 - 2	18.762 (0.001)	15.671 (0.001)	38.324 (0.001)
Montdardier M6	<2	19.298 (0.002)	17.728 (0.001)	38.186 (0.002)
Sanguinède S1	<2	18.936 (0.001)	15.668 (0.001)	38.112 (0.001)
	<0.4	18.984 (0.001)	15.676 (0.001)	38.130 (0.001)
	0.4 - 2	18.984 (0.001)	15.677 (0.001)	38.130 (0.001)

Discussion

The K-Ar ages support crystallization of several generations of illite during distinct thermal episodes in the southeastern mining district of the French Central Massif, in ore-bearing and barren Cambrian, Permian, Triassic and Jurassic sediments. This evolutionary picture occurred along the main Cévennes faulting system that expectedly acted as a circulation drain for Pb-Zn mineralizing fluids; some of the samples having been impregnated several times. The different thermal events dated here by illite K-Ar can also be postulated on the basis of local and regional geochronological studies, as hydrothermal activity could be identified and dated in plutonic and sedimentary rocks at many West-European sites. Furthermore, the μ-values of the illite Pb system indicate a crustal composition for the migrating fluids that were necessarily hot and of hydrothermal origin, at least during the 191 ± 41 Ma event.

The geologic meaning of the K-Ar data on illite

At the Lodeve-Les Malines regional scale

The age identities among the two finer size fractions of the same sample corroborate geological meaningful ages as discussed by Clauer, Chaudhuri (1998) who illustrated this behavior by a “bench-type” sketch with the same age necessarily of geological meaning for the finer fractions and an older age geologically meaningless for the coarser fraction. Depending on the deposition timing of the studied sediments, Cambrian, Permian, Triassic and Jurassic, and if the fine (<0.4 μm) fractions consist mainly of authigenic illite, the following multi-episodic tectonic-thermal activity can be postulated at 285 ± 5 Ma in the pyroclastic feldspars and Cambrian sediments of Les Malines deposits as a post-Variscan thermal episode. This occurs at 240 ± 20 Ma mainly in the Cambrian sediments from Les Malines area and at 185 ± 15 Ma mainly

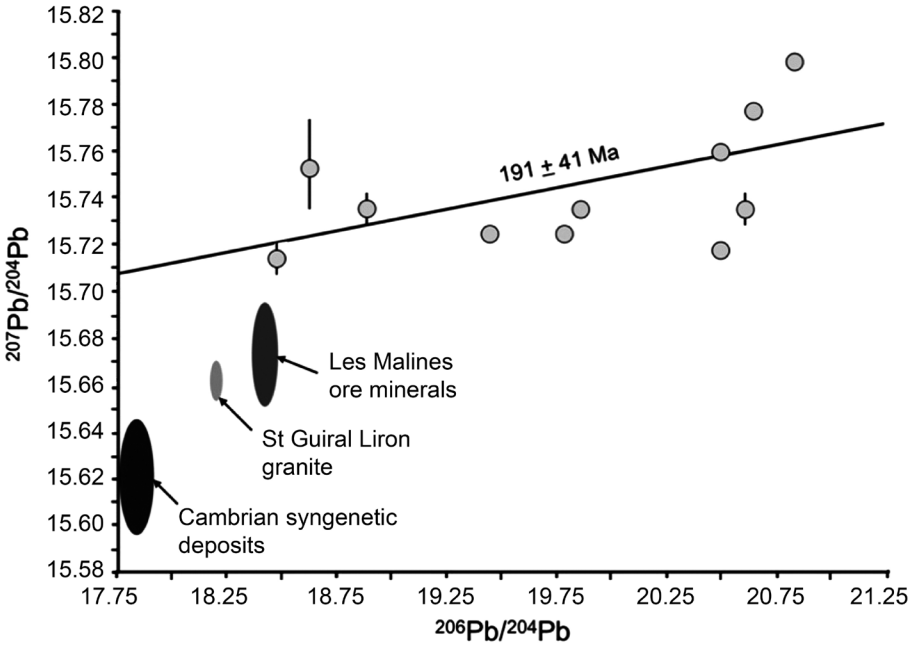

Fig. 4 *Pb-Pb errorchron of the clay residues from Cambrian size fractions relative to the Cambrian syngenetic deposits, the St Guiral-Licon granite and Les Malines Triassic and Liassic ores (Lancelot et al, 1971; Lancelot, Vella 1989; Le Guen et al. 1991; Lancelot et al, 1995).*

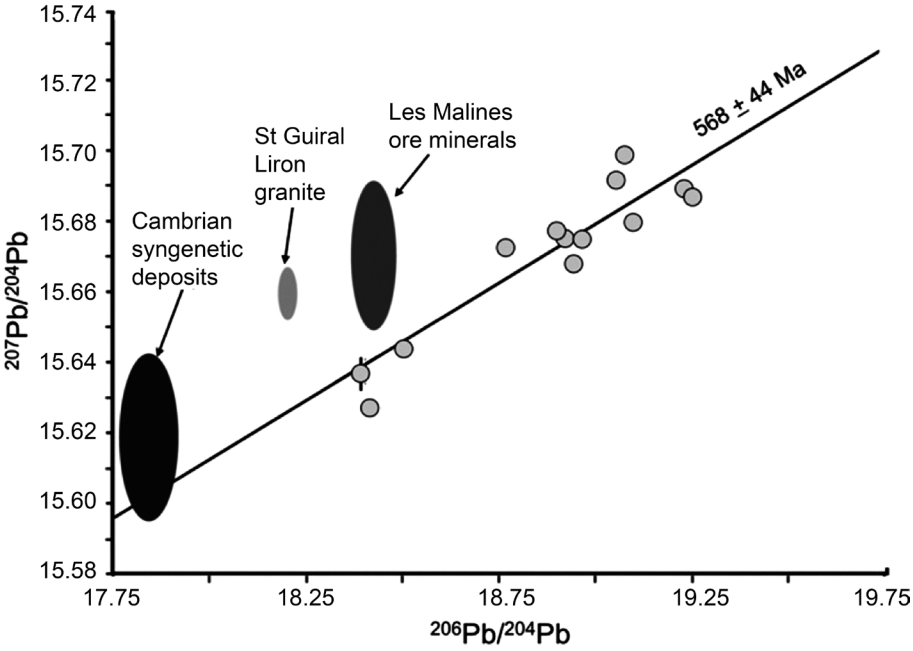

Fig. 5 *Pb-Pb errorchron of the clay leachates from analyzed Cambrian size fractions relative to the Cambrian syngenetic deposits, the St Guiral-Licon granite and Les Malines Triassic and Liassic ores, also reported in Fig. 4.*

in the Jurassic sediments of Trèves-Lanuejols as well as by Pb-Pb in the illite of Montdardier´s mine. The last two events are reflected at 140 ± 10 Ma in the Permian sediments of the Mas Lavayre district, and at 105 ± 5 Ma in the fault gouge of the Saint-Julien fault as well as in the Mas Lavayre mine (Mendez Santizo 1991).

In a complementary publication, Brockamp, Clauer (2013) studied diagenetic processes, hydrothermal alteration, as well as their timing in illite-rich size fractions of Permian shales close to the Lodève U-deposits. Illite with a mean K-Ar age of about 260 Ma is the predominant mineral in the shales. It is of early diagenetic origin relative to deposition and apparently formed directly from deposited pyroclastic materials in a lagoonal to deltaic environment under semi-arid conditions. Albite and a first generation of K-feldspar developed by replacement of analcime, growing only in the lagoonal environment that favored also early diagenetic dolomite formation at the expense of calcite. The hydrothermally altered shales next to the U-deposit contain authigenic quartz, Fe-chlorite, and a younger K-feldspar generation with K-Ar ages clustered around 220 Ma (Triassic), although Jurassic and Cretaceous ages were also obtained. This Triassic to Cretaceous age spectrum reflects similar periodic illitization episodes. The hydrothermal temperatures were below 200 °C as the early diagenetically formed illite is only partially reset. The Triassic hot fluids ascended along faults into the northern part of the Lodève basin during an initial rifting of the nearby evolving western Tethys Ocean. Further fluid pulses were recorded at Lodève during the opening of the North Atlantic and separation of Europe from Africa (Jurassic/Cretaceous). The Lodève district was apparently intruded by hot fluids of crustal origin for a long time, during successive episodic pulses.

In summary, the early thermal event detected at 285 ± 5 Ma in the pyroclastic feldspars and in a Montdardier Cambrian sediment was expectedly not recorded in the Permian sediments that were deposited afterwards. The 240 ± 20 Ma episode was recorded by pyroclastic feldspars of Permian age, as well as by Cambrian sediments at Montdardier and by Permian sediments at Lodève and Mas Lavayre. If the volcanic activity does not imply some regional abnormal thermal conditions in the Permian sediments, it is not the same for the imprint in sediments of varied stratigraphic age at different locations. A paleothermometric study of fluid inclusions in quartz and authigenic clay material indicated that bi-phase aqueous inclusions of quartz from faults in the Upper Permian yield homogenization temperatures from 60 to 300 °C (Staffelbach et al. 1987; Mendez Santizo et al. 1991). Most of the inclusions yield homogenization temperatures from 150 to 300 °C with a maximum frequency at 170 - 180 °C in the major fractures such as that of the Saint-Julien district. The homogenization temperatures above 240 °C were obtained on inclusions from quartz that have melting temperatures corresponding to salinities between 16.5 and 12 wt. % eq. NaCl. The fractionation coefficient of Co between pyrite and pyrrhotite being temperature dependent (Bezmen et al. 1975) yielded for the pyrite-pyrrhotite association in the Saint-Julien fault the temperatures 280 ± 6 °C for the gouge material and 242 ± 22 °C for vein deposits in the host rocks. In fact, this latter temperature range does not match the diagenetic origin for the 260-Ma illite resulting from alteration of pyroclastic material in a lagoonal to deltaic environment under semi-arid conditions (Brockamp, Clauer 2013), unless the veins with the pyrite-pyrrhotite assemblage formed during a further fluid migration, for instance at the same time as in the Saint-Julien fault.

Various thermal conditions occurred necessarily in the studied host rocks of different stratigraphic ages and locations, including the fact that these diagenetic/hydrothermal conditions occurred soon after sediment deposition during Permian. The 185 ± 15 Ma episode appears to have had a climax impact in strata of various stratigraphic age, so it is demonstrated in Permian sediments at Lodève, Triassic at Ludes and Crozes, and Jurassic at Treves and Lanuejols, as well as in U-enriched veins at Rabejac (Lancelot, Vella 1989). Such a paroxysmal extensive activity was reported during the Rhaetian-Hettangian time in the Cévennes and western Alps, which corresponds to the development of the Ligurian Tethys (Lemoine et al. 1986; Dromart et al. 1998). The 105 ± 5 Ma Albian event is also well identified, as it corresponds to the onset of the first oceanic accretion in the Biscay Bay (Montadert et al. 1979), which is recorded in the Saint-Julien gouge fault (Mendez Santizo et al. 1991).

Of interest is the comparison of this timetable with the time schedule of the described tectonic features in the Lodève district by Laversanne (1976) and Santouil (1980). They identified an Autunian N20 compression, a Saxonian NS to N20 distension, an Ante-Triassic EW compression, a paroxysmal lower Liassic NS to N150 distension, a middle Cretaceous N60 distension, as well as two further events during the upper Cretaceous and the Oligocene. There is a good correspondence between the two independent timings of the regional tectonic-thermal activity in the district.

At the French Massif Central scale

The K-Ar ages of the illite-type clay material studied here fit well in the structural geologic framework of the regional post-Variscan plutonic evolution and the Liassic extensional tectonic episode along the Cévennes faulting system. The review of Lancelot et al. (1995) on ore occurrences in the French Massif Central also points to the regional evolution with an U pre-concentration episode at about 270 Ma in leucogranite veins percolated by fluids at 300 - 350 °C, as pitchblende at 188 ± 12 Ma (Respaut et al. 1991), uraninite at 172 ± 9 Ma (Léveque et al. 1988), and coffinite at about 100 Ma and even later at 35 - 40 Ma (Respaut et al. 1991) at Pierre Plantée. Some U concentration was detected at about 170 Ma in coffinite at Bertholène, which fits well the illite K-Ar ages. For instance, published K-Ar illite ages were reported between 220 and 160 Ma in the Lodève area (Bellon et al. 1974; Bonhomme, Millot 1978; Bonhomme et al. 1983). At Bernardan, six illite K-Ar ages average 161 ± 9 Ma (Clauer 2020) with four more values scattered between 240 and 185 Ma.

The same regional picture applies to fault gouges filled with clay minerals in plutonic and sedimentary rocks to the NW of the Central Massif (Cathelineau et al. 2004). There, the finest <0.2 µm fractions from deep fractures (>570 m) yield older ages from 272 to 253 Ma, and those from shallow-depth fractures yield younger K-Ar ages of 198 to 188 Ma, confirming the occurrence of two distinct tectonic-thermal episodes. These ages were considered to record the extensional episode accompanied by thermal anomalies related to the rifting of the central Atlantic Ocean. Alternatively, the other major tectonic-thermal episode, which affected the Gascogne Gulf in the Aquitaine Basin at ca. 120 Ma, was not detected. In a complementary study, Cathelineau et al. (2012) demonstrated that

migrating brines and seawater interacted with both the sedimentary cover and the basement in the Poitou High located to the northwestern edge of the French Massif Central, between the Aquitaine and Paris basins, at ages of 156 to 146 Ma based on K-Ar dating of illite and $^{40}Ar/^{39}Ar$ dating of associated feldspars. This hydrothermal activity induced significant dolomitization and silicification of the sediments, adularization of the basement, and local concentration of F-Ba (Pb-Zn) assemblages.

At the Western European scale

Further away from southeastern French Massif Central, Schleicher et al. (2006) reported Permian (270 to 250 Ma), Jurassic (180 to 160 Ma) and younger hydrothermal activities in the Soultz-sous-Forêts granite in the Rhine Graben. Other studies provided K-Ar illite ages of about 200 Ma (Liassic) in nearby Triassic sandstones of the Vosges Mountains-Rhine Graben structural setting, together with younger episodes (Clauer et al. 2008), and of about 190 Ma (Liassic) in Triassic sediments from central Paris Basin, again with younger episodes (Clauer et al. 1995). Further to the east in the Black Forest, Lippolt, Seibel (1991), and Lippolt, Kirsch (1994) reported Triassic and younger hydrothermal sericite crystallization episodes in altered gneissic plagioclases. A Late Jurassic hydrothermal alteration of Permian-Carboniferous sandstones was also reported in the Baden-Baden and Offenburg-Teinach troughs at temperatures of 240 - 290 °C and 150 - 210 °C, respectively (Zuther, Brockamp 1988; Brockamp et al. 2003). More Liassic hydrothermal activities were dated by Clauer et al. (1996) in sedimentary rocks of Western Europe and Northern Africa, as well as by Schaltegger et al. (1994) for an illite crystallization episode in northern Switzerland.

All these results confirm the occurrence of geographically widely dispersed, episodic hydrothermal activities in the different selected sites (Fig. 6). Illite crystallization often occurred in and nearby faulting systems that acted as drains for mineralizing fluids to migrate, favoring or not ore genesis. Alternatively, late-Variscan activity in plutonic basement rocks, especially of major cratonic basement of Western Europe, has been less reported.

Meaning of the illite Pb-Pb data in the regional evolution of the ore districts

The Pb isotopic composition of illite particles points to an approximate age of 191 ± 41 Ma, on the basis of an errorchron that suggests a partial Pb homogeneity. Despite this analytical problem, the obtained age confirms previously reported ages for nearby U deposits, namely a major recrystallization after a pre-concentration at about 270 Ma. Interestingly, the analytical characteristics of the errorchron are far from the Pb-isotopic field of the Cambrian syngenetic deposits, suggesting that the Pb trapped by the crystallizing illite during the 180 - 200 Ma hydrothermal episode was not from major local Pb reservoir. It is also away from the Pb field of the nearby St Guiral-Liron granite, which could have been another possible reservoir for the Pb trapped by the clay minerals (Fig. 4). These differences in the Pb-isotopic compositions of the illite crystallized at about 190 Ma, evidence a remote crustal origin for the Pb, including an interaction with hydrothermal fluids migrating in the local fault system.

The Pb-Pb data of the leachates consisting of Pb external to the illite particles adds further information to the evolution of the ore district. SEM observation showed illite particles coated by micrometric Pb-sulfide crystals, which were dissolved by dilute-acid leaching. The Pb-Pb isotopic data of the leachates, with an age of 568 ± 44 Ma for the errorchron, indicate that Pb of the dissolved ore crystals belongs to the large local Cambrian Pb reservoir. This is confirmed by the trajectory of the errorchron,

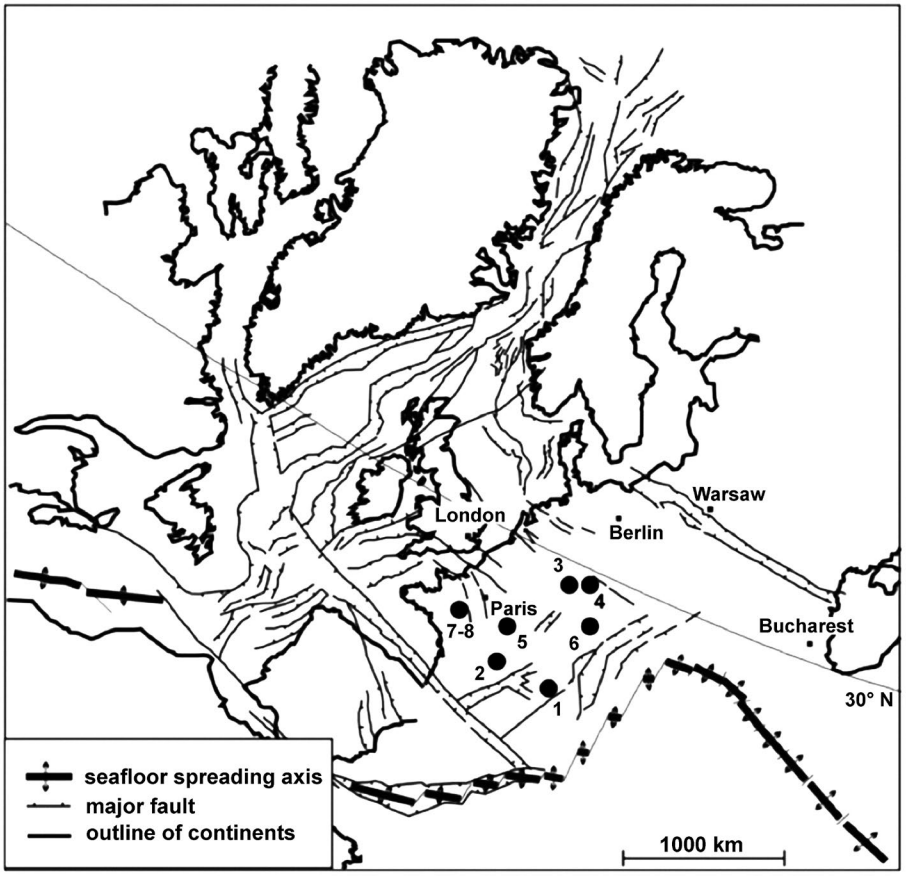

Fig. 6 *Tectonic framework of Europe during Jurassic time (after Muchez et al. 2005). The black dots locate: 1 = the Lodève-Les Malines Pb-Zn district, 2 = the Bernardan site, 3 = the Soultz-sous-Forêt granite, 4 = the Black Forest, 5 = the southern Paris Basin, 6 = northern Switzerland, 7 = the Poitou High, and 8 = the Charroux-Civray area.*

which cuts the Pb field of these ores, meaning in turn that the 190-Ma hydrothermal pulse did not modify the large reservoir (Fig. 5). In summary, Pb-isotopic determinations of barren illite-type minerals provide complementary information about the regional evolution of the ore district, the origin of the metals trapped by the authigenic clays, and the timing of the migrating Pb-loaded hydrothermal brines.

The meaning of isotopic dating of ores and associated minerals of metalliferous regions

On the basis of a large review of major basin-hosted ore deposits in Europe, Muchez et al. (2005) suspect that most of them formed in extensional settings. Where extension was pronounced and heat production elevated, the mineralizing fluids were expelled along extensional faults subsequently after having migrated through the sedimentary basin and the basement. This conclusion does not match with the regional location of illitization episodes in the Lodève-Les Malines district, which do not necessarily occur next to major tectonic or rifting regions (Fig. 6). Indeed, except for the aborted Rhine graben rifting, the results obtained in the southeastern French Massif and in Western Europe confirm the occurrence of two major episodes during the Upper Permian - Lower Triassic and during the Liassic times away from common tectonic/geodynamic activities, in rather quiescent areas where only re-activation of faulting systems can be identified. This specific absence of physical processes in the neighborhood of the metal deposits needs migration of hot -fluids in the continental crust, as metals were concentrated at specific places, not necessarily at each tectonic-thermal episode. A regional overview of the geochronologic results has indicated contemporary processes at the scale of Western Europe with U-F-Ba-Pb-Zn deposits. Many of such deposits were dated during Jurassic and Cretaceous episodes at 185 ± 15, 140 ± 10 and 105 ± 5 Ma, which supports a relationship between fluid movements and geodynamic events, but surprisingly away from the major activities.

In fact, the fluid-flow episodes dated by geochronology means and associated with ore minerals (UO_2 by U-Pb or fluorite by Sm-Nd) are often difficult to link with crustal processes at the scale of a province. It is, for instance, the case for the 1.6 to 1.3 Ga old U deposits in mid-Proterozoic basins of Canada and Australia (Hoeve, Quirt 1984; Kotzer, Kyser 1995), which is precisely a period almost devoid of nearby deformation structures and orogens, unless very remote events (more than 2000 km away) have local impacts. The brines that have extensively interacted with basement rocks at the microfracture scale, were subsequently channeled along earlier reactivated faults (Mercadier et al. 2010). Such results highlight the necessary re-evaluation of the remote effects of major geodynamic events on mass and heat transfers, in plutonic basements but also in sedimentary basins.

Conclusions

Illite-rich size-fractions of Cambrian, Permian, Triassic and Jurassic calcschists, shales and dolostones of the Pb -Zn ore district from southeastern French Massif Central were dated by the K-Ar method, and some were also dated by the Pb-Pb method after removal of the Pb external to the illite particles. The combined mineralogical, and K-Ar and Pb-Pb isotopic determinations allowed following conclusions:

(1) Illite K-Ar ages suggest crystallization episodes at about 280 ± 10, 240 ± 20 and 185 ± 5 Ma in the ore district, which were also reported at a larger regional scale. However, all these tectonic-thermal events were probably not monitored by Pb-mineralizing fluids, which seem to have contributed to illitization at 190 ± 40 Ma, probably at 140 ± 10 Ma and definitely at 105 ± 5 Ma, witnessed by ore Pb-Pb dating in faults, and during minor Cretaceous pulses.
(2) The Pb isotope data of the clay residues plot around a Pb-Pb errorchron giving an age of 191 ± 41 Ma, which is close to the Liassic age obtained by the K-Ar method. The significant scatter of the Pb-Pb data from clay residues suggests an incompletely equilibrated isotopic signature when incorporated into the illite structure during crystallization. Pb-isotopic determinations of barren illite-type minerals provide information about the regional evolution of the ore deposits, the origin of the metals trapped by these authigenic clays and the timing of the circulation of the hydrothermal fluids.
(3) The fluid events occurred within a segment of a continental margin away from main rift zones and from major deformation areas all over Western Europe. The lack of major geodynamic activities next to the metal deposits needs to consider periodic migrations of hot-fluid movements in the underneath continental crust, as metals were concentrated at specific places, but not necessarily at each tectonic-thermal pulse recorded by illite.
(4) The tectonic-thermal history of the Lodève-Les Malines ore district confirms repetitive geodynamic re-activations of previously occurring events with effects on local mass and heat transfers in the plutonic basements, as well as in the sedimentary sequences.

Acknowledgements

We would like to thank Ray Wendling, R. Winkler for technical assistance during the K-Ar determinations, Rob Wendling for the clay extractions and J. Samuel for the ICP-MS determinations, all of the Centre de Géochimie de la Surface at the Université Louis Pasteur of Strasbourg. We extend also our sincere thanks to N. Clauer and W. Todt for access to their laboratories and mass spectrometers at the Centre de Géochimie de la Surface in Strasbourg, France, and Max-Planck Institute of Mainz, Germany, respectively. The review of two anonymous researchers and the editorial handling of Jiří Sejkora is especially acknowledged.

References

Bell K (1985) Geochronology of the Carswell area, northern Saskatchewan. In: Lainé R, Alonso D, Svab M (eds.) The Carswell structure uranium deposits, Saskatchewan. Geol Assoc of Canada, Spec Pap 29: 33-45

Bellon H, Ellenberger F, Maury R (1974) Sur le rajeunissement de íllite des pélites saxoniennes du basin de Lodève. C R Acad Sci Fr 278: 413-415

Bernard AJ (1958) Contribution à létude de la province métallifère sous-cévenole. PhD thesis Nancy Univ and Mém Sci Terre Nancy 7: 123-403

Bezmen NI, Tikhomirova VI, Kosogova VP (1975) Pyrite-pyrrhotite geothermometer: distribution of nickel and cobalt. Geokhimiya 5: 700-714

Bonhomme M, Millot G (1978) Diagenèse généralisée du Jurassique moyen (170-160 Ma) dans le basin du Rhône inférieur jusqu´ á la bordure de Cévennes (France). C R Acad Sci Fr 304: 431-434

Bonhomme M, Bühmann D, Besnus Y (1983) Reliability of K-Ar dating of clays and silicifications associated with vein mineralizations in Western Europe. Geol Rundsch 72: 105-117

Bonhomme MG, Thuizat R, Pinault Y, Clauer N, Wendling A, Winkler R (1975) Méthode de datation Potassium-Argon. Appareillage et technique. Note technique Inst. Géol Strasbourg 3, 72: 105-117

Bray CJ, Spooner ETC, Hall CM, York D, Bills TM, Krueger HW (1987) Laser probe $^{40}Ar/^{39}Ar$ and conventional K-Ar dating of illites associated with the McClean unconformity-related uranium deposits, north Saskatchewan, Canada. Can J Earth Sci 24: 10-23

Brockamp O, Clauer N (2013) Hydrothermal and unexpected diagenetic alteration in Permian shales of the Lodève epigenetic U-deposit of southern France, traced by K–Ar illite and K-feldspar dating. Chem Geol 357: 18-28

Brockamp O, Clauer N, Zuther M (2003) Authigenic sericite record of a fossil geothermal system: the Offenburg trough, central Black Forest, Germany. Int J Earth Sci 92: 843-851

Brockamp O, Zuther M, Clauer N (1987) Epigenetic-hydrothermal origin of the sediment-hosted Muellenbach uranium deposit, Baden-Baden, W-Germany. Monograph Series on Mineral Deposits 27: 87-98

Cameron AE, Smith DH, Walker RL (1969) Mass spectrometry of nanogram-size samples of lead. Anal Chem 41, 525-526.

Cathelineau M, Boiron MC, Fourcade S, Ruffet G, Clauer N, Belcourt O, Coulibaly Y, Banks DA, Guillocheau F (2012) A major Late Jurassic fluid event at the basin/basement unconformity in western France: $^{40}Ar/^{39}Ar$ and K-Ar dating, fluid chemistry, and related geodynamic context. Chem Geol 322-323: 99-120

Cathelineau M, Fourcade S, Clauer N, Buschaert S. Rousset D, Boiron MC, Meunier A, Lavastre V, Javoy M (2004) Dating multistage paleofluid percolations: A K-Ar and ^{18}O study of fracture illites from altered Hercynian plutonites at the basement/cover interface (Poitou High, France). Geochim Cosmochim Acta 68: 2529-2542

Chahi A, Clauer N, Toulkeridis T, Bouabdelli M (1999) Rare earth element distribution as tracer of the genetic relationship between smectite and palygorskite of marine phosphorites. Clay Min 34: 419-427

Charef A, Sheppard SMF (1988) The Malines Cambrian carbonate-shale-hosted Pb- Zn deposit, France: Thermometric and isotopic (H, O) evidence for pulsating hydrothermal mineralization. Miner Depos 23: 86-95

Clauer N (2020) The post-Variscan tectonic-thermal activity in the southeastern metalliferous province of the French Massif Central revisited with K-Ar ages of illite. Ore Geol Rev 117: 103300

Clauer N, Chaudhuri S (1992) Indirect dating of sediment-hosted ore deposits: Promises and problems. In: Clauer N, Chaudhuri S (Eds.) Isotopic signatures and sedimentary records. Lecture Notes in Earth Sciences, Springer Verlag, Heidelberg 43: 361-388

Clauer N, Chaudhuri S (1995) Clays in crustal environments. Isotope dating and tracing. 1-359, Springer Verlag, Heidelberg

Clauer N, Chaudhuri S (1998) Isotopic dating of very low-grade metasedimentary and metavolcanic rocks: techniques and methods. In: Frey M, Robinson D (eds.) Low-grade metamorphism. 202-226. Blackwell Science, Oxford

Clauer N, Chaudhuri S, Kralik M, Bonnot-Courtois C (1993) Effects of experimental leaching on Rb-Sr and K-Ar isotopic systems and REE contents of diagenetic illite. Chem Geol 103: 1-16

Clauer N, Chaudhuri S, Lewan MD, Toulkeridis T (2006): Effect of thermal maturation on the K–Ar, Rb–Sr and REE systematics of an organic-rich New Albany Shale as determined by hydrous pyrolysis. Chem Geol 234: 169-177

Clauer N, Ey F, Gauthier-Lafaye F (1985) K-Ar dating of different rock types from the Cluff Lake uranium ore deposits (Saskatchewan-Canada). In: The Carswell structure uranium deposits, Saskatchewan. Special Paper Geol Assoc Canada 29: 47-53

Clauer N, Liewig N, Ledesert B, Zwingmann H (2008) Evolution of Triassic sandstones from Vosges Mountains-Rhine Graben structural setting, NE France, based on K-Ar illite dating: Local and regional geodynamic implications. Clay Min 43: 363-379

Clauer N, Liewig N, Pierret MC, Toulkeridis T (2003): Crystallization conditions of fundamental particles from mixed-layer illite-smectite of bentonites based on isotopic data (K-Ar, Rb-Sr and $\delta^{18}O$). Clay Clay Miner 51: 664-674

Clauer N, O´Neil JR, Furlan S (1995) Clay minerals as records of temperature conditions and duration of thermal anomalies in the Paris Basin, France. Clay Min 30: 1-13

Clauer N, Toulkeridis T, Srodon J, Uysal T, Aubert A (2020). K-Ar and Rb-Sr ages of nanometer-sized smectite-rich illite/smectite mixed-layers from bentonite beds of the Campos Basin (Rio de Janeiro State, Brazil). Clay Clay Miner, DOI 10.1007/s42860-020-0087-5

Clauer N, Weber F, Gauthier-Lafaye F, Toulkeridis T, Sizun JP (1997) Mineralogical, geochemical (REE), and isotopic (K-Ar, Rb-Sr, $\delta^{18}O$) evolution of the clay minerals from faulted, carbonate-rich, passive paleomargin of Southeastern Massif Central, France. J Sedim Res 67: 923-934

Clauer N, Zwingmann H, Chaudhuri S (1996) Isotope (K-Ar and oxygen) constraints on the extent and importance of the Liassic hydrothermal activity in western Europe. Clay Min 31: 301-318

Connan J, Orgeval JJ (1977) Un exemple d´application de la géochimie organique en métallogénie : la mine des Malines (Gard, France). Bull Cent Rech Explor Prod Elf Aquitaine, 1: 59-105

Dromart G, Allemand P, Quiquerez A (1998) Calculating rates of syndepositional normal faulting in the western margin of the Mesozoic Subalpine Basin (south-east France). Bas Res 10: 235-260

Fogliérini F, Bernard A, Verraes G (1980) Le gisement Zn-Pb des Malines (Gard). Gisement Français Fasc E5 26e CGI, Dél Gén Rech Scien Techn 1-56

Goldfarb RJ, Bradley D, Leach DL (2010). Secular variation in economic geology. Econ Geol 105(3): 459-465

Halliday AN, Mitchell JG (1983) K-Ar ages of clay concentrates from Irish ore- bodies and their bearing on the timing of mineralization. Trans Roy Soc Edinburgh Earth Sci 74: 1-14

Halter G, Sheppard SMF, Weber F, Clauer N, Pagel M (1987) Radiation-related retrograde hydrogen isotope and K-Ar exchange in clay minerals. Nature 330: 638-641

Hamet J, Mattauer M (1977) Age hercynien determine par la méthode ^{87}Rb-^{87}Sr du granite de l´Aigoual. Conséquences structurales. C R Somm Soc Géol Fr 2: 80-84

Hoeve J, Quirt D (1984) Uranium mineralization and host rock alteration in relation to clay mineral diagenesis and evolution of the Middle-Proterozoic Athabasca Basin. Saskatch Res Coun Northern Saskatchewan Canada Report 187

Holliger P, Pagel M, Pironon J (1989) A model for ^{238}U radioactive daughter loss from sediment-hosted pitchblende deposits and the Late Permian-Early Triassic depositional U-Pb age of the Müllenbach uranium ore (Baden-Württemberg, F.R.G.). Chem Geol (Isot Geosci Sect) 80: 45-53

Ineson PR, Mitchell JC, Vokes FM (1975) K-Ar dating of epigenetic mineral deposits: An investigation of the Permian metallogenic province of the Oslo region, Southern Norway. Econ Geol 70: 1426-1436

Kotzer TG, Kyser TK (1995) Petrogenesis of the Proterozoic Athabasca basin, Northern Saskatchewan, Canada, and its relation to diagenesis, hydrothermal uranium mineralization and paleohydrogeology. Chem Geol 120: 45-89

Krogh TE (1973) A low-contamination method for hydrothermal decomposition of zircon and extraction of U and Pb for isotopic age determinations. Geochim Cosmochim Acta 9: 1-32

Kübler B (1968) Evaluation quantitative du métamorphisme par la cristallinité de l'illite. Bulletin Centre de Recherche de Pau, SNPA: 285-397

Kübler B (1997) Concomitant alteration of clay minerals and organic matter during burial diagenesis. In: Paquet H, Clauer N (eds.). Soils and sediments: 327-362. Springer Verlag

Kyser K, Hiatt E, Renac C, Durocher K, Holk G, Deckart K (2000) Diagenetic fluids in paleo- and meso-Proterozoic sedimentary basins and their implications for long protracted fluid histories. In: Kyser K (ed.) Fluids and basin evolution. Mineral Assoc Canada Short Course Series 28: 225-262

Lancelot J, Briqueu L, Respaut JP, Clauer N (1995) Géochimie isotopique des systèmes U-Pb/Pb-Pb et evolution polyphasée de gîtes d´uranium du Lodévois et du sud du Massif Central. Chron Rech Min 521: 3-18

Lancelot J, Sarazin G, Allegre CJ (1971) Composition isotopique du plomb et du soufre des galènes liées aux formations sédimentaires interprétations géologiques et géophysiques. Contr Miner Petrolog 32(4): 315-333

Lancelot J, Vella V (1989) Datation U-Pb liasique de la pechblende de Rabejac. Mise en evidence d´une préconcentration uranifère permienne dans le basin de Lodève (Hérault). Bull Soc Geol Fr 8: 309-315

Laverret E, Clauer N, Fallick A, Patrier P, Beaufort D, Quirt D, Kister P, Bruneton P (2010) K-Ar, $\delta^{18}O$ and δD tracing of illitization within and outside the Shea Creek uranium prospect, Athabasca Basin, Canada. Appl Geochem 25: 856-871

Laversanne J (1976) Sédimentation et mineralization uranifère du Permien de Lodève. PhD Thesis Univ Orsay

Le Guen M, Combes PJ (1988) Typologie des minéralisations plombo-zincifères associées au Bathonien des Malines (Gard, France). Doc Bur Rec Géol Min 135: 821-841

Le Guen M, Lancelot JR (1989) Origine du Pb-Zn des minéralisations du Bathonien sud-cévenol: apport de la géochimie isotopique comparée des galènes, de leur encaissant et du socle. Chron Rech Min 495: 31-36

Le Guen M, Orgeval JJ, Lancelot J (1991) Lead isotope behaviour in a polyphased Pb-Zn ore deposit, Les Malines (Cévennes, France). Miner Depos 26: 150-188

Lee MJ, Brookins DG (1978) Rubidium-strontium minimum ages of sedimentation, uranium mineralization, and provenance, Morrison Formation (Upper Jurassic), Grants mineral belt, New Mexico. Amer Assoc Petrol Geol Bull 62: 1673-1683

Lemoine M (1984) La marge occidentale de la Téthys Ligure et les Alpes occidentales. In : Boillot G, Montadert L, Lemoine M, Biju-Duval B. (eds.) Les marges continentales actuelles et fossiles autour de la France: 125-248. Masson, Paris

Lemoine M, Bas T, Arnaud-Vanneau A, Arnaud H, Dumont T, Gidon M, Bourbon M, de Graciansky PC, Rudkiewicz JL, Megard-Galli J, Tricart P (1986) The continental margin of the Mesozoic Tethys in the Western Alps. Mar Petrol Geol 3: 179-199

Lévêque MH, Lancelot J, George E (1988) The Bertholène uranium deposit - Mineralogical characteristics and U-Pb dating of the primary U mineralization and its subsequent remobilization: Consequences upon the evolution of the U deposits of the Massif Central, France. Chem Geol 69: 147-163

Lippolt HJ, Kirsch H (1994) Isotopic investigation of Post-Variscan plagioclase sericitation in the Schwarzwald gneiss massif. Chem Erde 54: 179 - 198

Lippolt HJ, Siebel W (1991) Evidence for multi-stage alteration of Schwarzwald lamprophyres. Eur J Miner 3: 587-601

Macquar JC (1970) Le Trias. Bull Bur Rech Géol Min 2 II 1: 27-65

Mendez Santizo J (1990) Diagenèse et circulations de fluids dans le gisement d´uranium de Lodève (Hérault). PhD thesis. Univ Strasbourg

Mendez Santizo J, Gauthier-Lafaye F, Liewig N, Clauer N, Weber F (1991) Existence d'un hydrothermalisme tardif dans le bassin de Lodève (Hérault). Arguments paléothermométriques et géochronologiques. C R Acad Sci Paris 312: 739-745

Mercadier J, Richard A, Boiron MC, Cathelineau M, Cuney M (2010) Migration of brine in the basement rocks of the Athabasca Basin through microfracture networks (P-Patch U deposit, Canada). Lithos 115: 121-136

Merignac C, Cuney M (1999) Ore deposits of the French Massif central: Insight into the metallogenesis of the Variscan collision belt. Miner Depos 34: 472-504

Michaud JG (1970) Gisements de Pb-Zn du Sud du Massif Central français (Cévennes- Montagne Noire) et caractéristiques géologiques de leur environnement. Bull Cent Rech Expl Prod Elf Aquitaine 3: 335-380

Miller DS, Kulp JL (1963) Isotopic evidence on the origin of the Colorado Plateau uranium ores. Geol Soc Amer Bull 75: 609-630

Misi A, Iyer SS, Silva Coelho CE, Tassinari CCG, Franca-Rocha WJS, Rocha Gomes AS, Cunha IA, Toulkeridis T, Sanches AL (2000) A metallogenic evolution model for the lead-zinc deposits of the Meso and Neoproterozoic sedimentary basins of the São Francisco Craton, Bahia and Minas Gerais, Brazil. Rev Brasil Geoci 30 (2): 302-305

Montadert L, Roberts DG, de Charpal O, Guennoc P (1979) Rifting and subsidence of the northern continental margin of the Bay of Biscaye. In: Montadert L, Roberts DG et al (Eds.) Init Rep Deep Sea Drill Proj 48: 1025-1060. US Govern Print Office, Washington

Muchez P, Heijlen W, Banks D, Blundell D, Boni M, Grandia F (2005) Extensional tectonics and the timing and formation of basin-hosted deposits in Europe. Ore Geol Rev 27: 241-267

Nasraoui M, Toulkeridis T, Clauer N, Bilal E (2000) Differentiated hydrothermal and meteoric alterations of the Lueshe carbonatite complex (NE of Congo Democratic Republic) identified by a REE study combined with a sequential acid-leaching experiment. Chem Geol 165: 109-132

Nier AO (1950) A redetermination of the relative abundances of the isotopes of carbon, nitrogen, oxygen, argon and potassium. Phys Rev 77: 789-793

Odin GS and 35 collaborators (1982) Interlaboratory standards for dating purposes. In: Odin G.S. (ed.) Numerical dating in stratigraphy. 123-158. J Wiley & Sons Ltd

Orgeval JJ (1976) Les remplissages karstiques minéralisés : exemple de la mine des Malines (Gard, France). Mém H Sér Soc Géol Fr 7: 77-85

Platt JD (1993) Controls on clay mineral distribution and chemistry in the Early Permian Rotliegend of Germany. Clay Min 28: 393-416

Polito PA, Kyser TK, Jackson MJ (2006) The role of sandstone diagenesis and aquifer evolution in the formation of uranium and zinc-lead deposits, southern McArthur Basin, Northern Territory, Australia. Econ Geol 101: 1189-1209

Rajesh HM (2008) Mapping Proterozoic unconformity-related uranium deposits in the Rockhole area, Northern Territory, Australia using landsat ETM+. Ore Geol Rev 33(3): 382-396

Ramboz CC (1989) Conditions of fluid circulation in rifts: comparison between the Subalpine Basin and the Central Red Sea. 202. EUG Strasbourg Terra Cognita Abstracts 1

Respaut JP, Cathelineau M, Lancelot J (1991) Multistage evolution of the Pierres Plantées uranium ore deposit (Margeride, France): evidence from mineralogy and U-Pb systematics. Eur J Miner 3: 85-103

Romer RL (2001) Lead incorporation during crystal growth and the misinterpretation of geochronological data from low-$^{238}U/^{204}Pb$ metamorphic minerals. Terra Nova 13: 258-263

Santouil G (1980) Tectonique et microtectonique comparée de la distension permienne et de l´évolution post-triasique dans les basins de Lodève, Saint-Affrique et Rodez (France SE). Master thesis. Univ Montpellier II

Schaltegger U, Stille P, Rais N, Piqué A, Clauer N (1994) Nd and Sr isotopic dating of diagenesis and low-grade metamorphism of argillaceous sediments. Geochim Cosmochim Acta 58: 1471-1481

Schleicher A, Warr LN, Kober B. Laverret E, Clauer N (2006) Episodic mineralization of hydrothermal illite in the Soultz-sous-Forêts granite (Upper Rhine Graben, France). Contr Miner Petrol 152: 349-364

Stacey JS, Kramers JD (1975) Approximation of terrestrial lead isotopes evolution by a two-stage model. Earth Planet Sci Lett 26: 207-221

Staffelbach C, Mendez Santizo J, Horrenberger JC, Ruhland M, Weber F (1987) Metallogenesis of uranium deposits. AIEA Proceed Techn Commit Meet Vienna 9: 119-135

Steiger RH, Jäger E (1977) Subcommission on geochronology: convention on the use of decay constants in geo- and cosmochronology. Earth Plan Sci Lett 36: 359-362

Todt W, Cliff RA, Hanser A, Hofmann AW (1996) Evaluation of a ^{202}Pb-^{205}Pb double spike for high-precision lead isotope analysis. In: Basu A. (ed.) Earth processes reading the isotopic code: 429-437. Geophys Monogr 95. Amer Geophys Union Washington

Toulkeridis T, Clauer N, Kröner A (1996) Chemical variations in clay minerals of the Archean Barberton Greenstone Belt (South Africa). Precambr Res 79: 195-207

Toulkeridis T, Clauer N, Chaudhuri S, Goldstein SL (1998) Multi-method (K-Ar, Rb-Sr, Sm-Nd) dating of bentonite minerals from eastern United States. Basin Res 10: 261-270

Toulkeridis T, Goldstein SL, Clauer N, Kröner A, Lowe DR (1994) Sm-Nd dating of Fig Tree clay minerals of the Barberton Greenstone Belt, South Africa. Geology 22: 199-202

Turpin L, Clauer N, Forbes P, Pagel M (1991) U-Pb, Sm -Nd and K-Ar systematics of the Akouta uranium deposit, Niger. Chem Geol Isot Geosc Sect 87: 217-230

Verraes G (1983) Etude monographique du district minier des Malines et de ses environs (province sous cévenole, France). PhD thesis Univ Montpellier

Vialette Y, Sabourdy G (1977) Age du granite de l´Aigoual dans le massif des Cévennes (France). C R Somm Soc Géol France 3: 130-132

Wilson MR, Kyser TK, Mehnert HH, Hoeve J (1987) Changes in the H-O-Ar isotope composition of clays during retrograde alteration. Geochim Cosmochim Acta 51: 869-878

Zhao B, Clauer N, Robb LJ, Zwingmann H, Toulkeridis T, Meyer MF (1999) K-Ar dating of micas from the Witwatersrand Basin, South Africa: timing of post-depositional alteration and gold mineralization. Mineral Petrol 66: 149-170

Zuther M, Brockamp O (1988) The fossil geothermal system of the Baden-Baden trough (Northern Black Forest, F.R. Germany). Chem Geol 71: 337-353